Published in final edited form as:
Nat Genet. 2018 July ; 50(7): 1021–1031. doi:10.1038/s41588-018-0149-1.

Gorab is a Golgi protein required for structure and duplication of *Drosophila* centrioles

Levente Kovacs[1], **Jennifer Chao-Chu**[#1,3], **Sandra Schneider**[#1], **Marco Gottardo**[2,4], **George Tzolovsky**[2,5], **Nikola S. Dzhindzhev**[1], **Maria Giovanna Riparbelli**[2], **Giuliano Callaini**[2], and **David M. Glover**[1,*]

[1]Department of Genetics, University of Cambridge, Cambridge, United Kingdom

[2]Department of Life Sciences, University of Siena, Siena, Italy

[#] These authors contributed equally to this work.

Abstract

We demonstrate that a *Drosophila* Golgi protein, Gorab, is present not only in the trans-Golgi but also in the centriole cartwheel where, complexed to Sas6, it is required for centriole duplication. In addition to centriole defects, flies lacking Gorab are uncoordinated due to defects in sensory cilia, which lose their 9-fold symmetry. We demonstrate the separation of centriole and Golgi functions of *Drosophila* Gorab in two ways: First, we have created Gorab variants that are unable to localize to trans-Golgi but can still rescue the centriole and cilia defects of *gorab* null flies. Second, we show that expression of C-terminally tagged Gorab disrupts Golgi functions in cytokinesis of male meiosis, a dominant phenotype overcome by mutations preventing Golgi targeting. Our findings suggest that during metazoan evolution, a Golgi protein has arisen with a second, apparently independent, role in centriole duplication.

[*]Correspondence to: dmg25@cam.ac.uk.
[3]**Present addresses:** School of Biomedical Sciences, The University of Hong Kong, Hong Kong
[4]**Present addresses:** Alexander von Humboldt Foundation Fellow, Center for Molecular Medicine and Institute for Biochemistry of the University of Cologne, Cologne, Germany
[5]**Present addresses:** Carl Zeiss Microscopy Ltd, ZEISS Group, Cambridge, United Kingdom

Author Contribution

L.K. contributed to planning experiments, fluorescent microscopy, Drosophila genetics, super resolution microscopy, cell culture work, data analysis and writing manuscript; J.C.C contributed to antibody generation, mass spectrometry, Drosophila genetics, fluorescent microscopy; S.S. contributed to mass spectrometry, in vitro interaction studies, protein structure analysis, cell culture work; M.G. contributed to electron microscopy; G.T. contributed to super resolution microscopy; N.S.D. contributed to planning experiments, data analysis; M.G.R. contributed to electron microscopy; G.C. contributed to electron microscopy; D.M.G. contributed to the conception and supervision of the study, planning experiments and writing the manuscript.

Competing Financial Interests Statement

The authors declare no competing interests.

Cited URLs

COILS server
https://embnet.vital-it.ch/software/COILS_form.html
Online Shapiro-Wilk test
http://sdittami.altervista.org/shapirotest/ShapiroTest.html

Data Availability Statement

The data that support the findings of this study are available from the corresponding author upon request.

Europe PMC Funders Author Manuscripts

Centrioles are at the core of centrosomes, required for cell-division fidelity, and at the base of cilia, fulfilling roles in motility and signalling. Their malfunction is associated with diseases ranging from cancer to ciliopathies and microcephaly. Canonical centriole duplication pathway components were genetically identified in *C.elegans*1 and through RNAi screens in *Drosophila*2,3. Centriole duplication requires Polo-like kinase 4, which phosphorylates Ana2/STIL enabling its recruitment to the procentriole site4 to interact with Sas6 upon procentriole formation5,6. The resulting structure reflects the symmetry of 9 interacting dimers of Sas6in the centriole's cartwheel. Cep135 (Bld10) is also required for cartwheel formation in *Chlamydomonas* and *Paramecium*7,8 and human Cep135 links Sas6 to Sas4 (CPAP)9, associated with and required for polymerisation of centriolar microtubules (MTs)10–12. Although the centriole reaches its full length by the end of G2, it cannot duplicate or organize pericentriolar-material (PCM) until it passes through mitosis13,14. This requires Cep135 to recruit Ana1 in *Drosophila* (CEP295 in human cells), and in turn Asterless/Cep152and pericentrin-like protein15. This process of centriole to centrosome conversion enables the daughter centriole to recruit Plk4, as a partner of Asterless/Cep152, and PCM components that organise cytoplasmic MTs.

In interphase, the centrosome is found in the vicinity of the Golgi, the heart of secretory pathways and key for vesicular trafficking. Golgi positioning and vesicle trafficking rely on cytoplasmic MTs organized by Golgi-associated AKAP450 (counterpart of pericentrin), the *cis*-Golgi protein GM130, the *trans*-Golgi CLASPs (cytoplasmic-linker-associated-proteins), and additional components of a multiprotein complex16–18. Interphase cells can also utilise the mother centriole to template cilia formation. The Golgi participates in this process by providing membrane for the cilium and the ciliary pocket adjacent to the mother centriole19–21. In mammalian cells, this requires golgin GMAP-210, which interacts with the intraflagellar-transport complex protein, IFT-20, required for ciliogenesis22,23. Such links between centrosome and Golgi are only beginning to be explored and require further study.

Although Sas6 adopts a 9-fold symmetrical structure *in vitro*, Sas6 alone cannot confer 9-fold symmetry on the centriole *in vivo*; mutations that disrupt Sas6'ssymmetry *in vitro*24 or that prevent its self-oligomerisation can still result in 9-fold symmetrical centrioles *in vivo*25. This suggests additional, yet unknown factors must help establish symmetry, raising the question of whether otherSas6-interacting proteins had been missed by earlier genome-wide screens. This led us to use proteomic approaches to search for additional *Drosophila* centriole components and the discovery of a new Sas6 partner, the fly counterpart of Golgi-associated Gorab. Human GORAB is mutated in gerodermia osteodysplastica, characterised by non-elastic skin and osteoporosis26. GORAB localises to the trans-Golgi membranes and interacts with SCYL1, which participates in the Golgi-ER trafficking of COPI vesicles27–30. We now show *Drosophila gorab* null mutants fail to duplicate centrosomes in embryos and diploid larval tissues and have defects in the 9-fold symmetry of cilia in neurosensory organs resulting in loss of coordination. We have created mutants of Drosophila Gorab that cannot localise to the Golgi but can still rescue centriolar phenotypes of the *gorab* null. We also generate a dominant negative Gorab with cytokinesis phenotypes that depend upon its Golgi localisation. Together our findings indicate *Drosophila* Gorab has dual roles at the Golgi and centriole.

Results

Gorab copurifies with Sas6 and is found at centrosomes and Golgi

Aiming to identify proteins recruited to the site of procentriole formation, we affinity purified Sas6 complexes from syncytial *Drosophila* embryos expressing GFP-tagged Sas6 and from cultured cells following induction of Protein-A-tagged Sas6. Surprisingly, no other centriole proteins were enriched in Sas6 pull-downs from embryos but we consistently identified the *CG33052* gene product (Table 1; Table S1). This complex persisted following high salt treatment(440mM NaCl) and was not affected by inhibiting protein phosphatases with okadaic acid suggesting it is a stable complex, insensitive to the protein phosphorylation state. Similarly, mass spectrometry of Sas6 complexes from cultured cells consistently identified CG33052. BLAST searches identified CG33052 as counterpart of human GORAB, mutated in the inherited disease gerodermia osteodysplastica, leading us to name *Drosophila* CG33052 as *Gorab*.

To further confirm that Sas6 and Gorab copurify as a complex, we established flyand cell lines expressing GFP-tagged Gorab. GFP-Gorab consistently co-purified with Sas6 as its sole centriole associated partner from syncytial embryos (Fig.1d; Table S2). Sas6 also co-purified with Gorab from cultured cells, irrespective of whether GFP-Gorab was expressed constitutively or from the inducible metallothionein promoter. However, in addition to Sas6, co-purified proteins also included the αCOP, β'COP and εCOP subunits of the cage-like COPI coatomer sub-complex and the γCOP and βCOP subunits of its adaptor subcomplex (Fig. 1d; Table S2). We did not detect COPI complex proteins in purifications of Sas6 or of GFP expressed in cultured cells. Nor did we detect COPI proteins associated with Gorab purified from syncytial embryos (Fig. 1d; Table S2), a stage prior to the onset of Golgi assembly31–33.

The centrosomal association of Gorab, suggested by its repeated copurification with Sas6, was confirmed in syncytial blastoderm embryos expressing a *Ubq-GFP-gorab* transgene, in which GFP-Gorab co-localised with the centriole protein, Asterless, in interphase (Fig. 1b) and mitosis (Fig. 1c). As the Golgi is not assembled at this stage, we did not detect the trans-Golgi Golgin245. Thus, at least in the absence of the Golgi, Gorab could be a *bone* fide centrosome component in partnership with Sas6.

We then determined the sub-cellular localisation of Gorab in cultured D.Mel-2 cells that have well established Golgi. Using antibodies against Gorab (Material and Methods) and counterstaining for markers of the cis- (GM130) and trans-Golgi (Golgin245), we found the greater part of all Gorab was associated with the trans-Golgi,like its human counterpart30 (Fig. 1e). However, Gorab was also associated with dPLP punctae indicating its presence at the centrosome independent of Golgin245 (Fig. 1f). Moreover, Gorab persisted at the centrosome in mitosis, when Golgi components become dispersed throughout the cell(Fig. S1a). Simlarly in cells of larval wing imaginal discs and central nervous system, transgenic GFP-Gorab was abundant on the trans-Golgi becoming dispersed during mitosis with a smaller fraction being stably associated with the centrosome (Fig. S1b and c).

Gorab directly binds Sas6 at the centriole core

The co-purification of Gorab and Sas6 and their centrosomal colocalisation raised the question of whether they interact directly. To address this, we expressed and purified GST-tagged Gorab from E.coli on Glutathione Sepharose 4B beads, which we incubated with ^{35}S-Met-labelled full-length Sas6, synthesised by coupled transcription-translation. This revealed direct binding of Sas6 to immobilized Gorab (Fig. 2a). To narrow down the interacting region, we made N- and C-terminally truncated S^{35}-labelled Sas6 peptides for use in similar binding experiments (Fig. 2b; Fig. S2). These experiments identified the 351 to 462 amino-acid segment of Sas6 as able to interact directly with Gorab.

Gorab's direct binding to Sas6 and its centrosomal localization suggested it should be associated with the centriole. Indeed, structured illumination microscopy (SIM) revealed Gorab co-localised with Sas6 in centriole zone I at the center of a ring of dPLP, which surrounds the mother centriole throughout the cell cycle. This dPLP ring is completed around the daughter centriole during mitosis in centriole to centrosome conversion. Gorab and Sas6 co-localised at mother and daughter centriole throughout the centrosome cycle and were recruited to the site of procentriole formation once mother and daughter disengaged in telophase (arrowheads in Fig. 2c). Thus Gorab and Sas6 associate at the core of the centriole from the very onset of its duplication.

gorab^{null}-derived embryos display mitotic defects due to centrosome loss

The above findings suggested a possible new function for this Golgi-associated protein that we addressed by generating *gorab* null mutants. We used CRISPR/Cas9 mutagenesis to simultaneously target the 5' and 3' ends and exon1 of the *gorab* gene (Online methods) and generated *gorab*^{1} (NT_037436.4:g.33_507del) and *gorab*^{2} (NT_037436.4:g.1_1097del), eliminating significant coding sequence and the ATG initiation codon (Fig.3a). We were unable to detect any Gorab protein in Western blots of whole fly extracts (Fig. 3c) of homozygotes of either allele leading us to consider both mutant alleles to be nulls.

Surprisingly, both homozygous *gorab*^{1} and *gorab*^{2} animals developed to adulthood. However, flies emerging at 25°C moved slowly and were uncoordinated and when raised at 29°C, were unable to climb or fly (Fig. 3d, video S1). Furthermore, embryos derived from *gorab* mutant females raised at 25°C failed to develop even when homozygous mutant mothers were mated to wild-type males (Fig. 3e). In contrast, *gorab*^{1} males were fertile suggesting the mutation did not affect spermatogenesis. A similar extent of female sterility and uncoordination was observed in flies trans-heterozygous for the two alleles, or when heterozygous to a large chromosomal deficiency, suggesting the defects result from the loss of Gorab function (Fig.3b). Accordingly, female fertility and coordination were restored by ubiquitous expression of a wild-type *gorab* transgene in the *gorab*^{1} mutant background (Fig. 3d, e). Thus, the primary consequences of loss of Gorab are female sterility and uncoordination.

Coordination defects have previously been attributed to defective neurosensory cilia of the femoral chordotonal organs (fChOs)34,35. Accordingly, we could rescue coordination defects but not the female sterility of *gorab*^{1} fliesby expressing *UAS-gorab* only in the

nervous system using the pan-neural driver *elav-GAL4*. This allowed us to recover coordinated adult females that generated sufficient embryos to analyse their development. Wild-type syncytial embryos undertake 13 rapid rounds of synchronous nuclear division cycles over a period of 2 hours. In contrast, only 50% of *gorab*^{1}-derived embryos showed any nuclear division but not beyond 5 or 6 rounds. Centrosomes, revealed by anti-centrosomin (Cnn) or anti-Asterless (Asl) staining, were dramatically reduced in number in *gorab*^{1}-derived embryos and were absent from the majority of mitotic spindle poles (Fig. 3f, g). The extensive disorganisation of *gorab*^{1}-derived embryos accords with the known requirement for centrosomes in the syncytial cycles. Thus, maternally provided Gorab is required for centrosome duplication and thereby the nuclear division cycles of the embryo. We also observed centrosome loss in*gorab*^{1} imaginal discs indicating Gorab is required for centrosome duplication in other diploid tissues (Fig. 3h).

Coordination defects of *gorab* flies reflect absence of daughter centrioles and loss of 9-fold symmetry in ciliary organs

As flies defective for centriole duplication lose coordination, we examined the fChOs whose ciliated neurons have basal bodies derived from centrioles (Fig. 4a). Wild-type fChOs have *Drosophila* pericentrin-like protein (dPLP) in mother and daughter centriole-derived structures, of which the mother forms the ciliary basal body. Transgenic GFP-rootletin identifies the ciliary rootlet connecting the basal bodies to the cell body and phalloidin staining reveals actin enveloping the two cilia of each scolopale. *gorab*^{1} mutant fChOs had highly disorganised ciliary rootlets often disconnected from basal bodies (Fig. 4a,b). dPLP associated structures were also disorganized in *gorab*^{1} mutants but ciliary structures were still present in the scolopale rods (Fig. 4a, b).

The two fChObasal bodies can be distinguished because only the proximal one (corresponding to a daughter centriole) has associated Centrobin36. However, 79.3 % (115/145) of basal bodies in *gorab*^{1} cilia had no Centrobin (Fig. 4c) and in the remaining 20.7 % (30/145)anti-Centrobin staining was very weak. This suggests a failure of centriole duplication prior to basal body formation. These defects were restored in *gorab*^{1} flies expressing a GFP-Gorab transgene (Fig. 4d).

To determine whether basal bodies of *gorab*^{1} ciliated neurons had other abnormalities we examined them in longitudinal and transverse section by electron microscopy (EM) (Fig. 4e, f). Longitudinal sections of fChOs revealed mother centrioles present in all distal basal bodies investigated (n=11)whereas proximal basal bodies were absent or reduced in accord with the lack of Centrobin signal (Fig. 4e).Transverse sections revealed striking defects in the radial symmetry of the remaining mother centriole-derived basal body in *gorab*^{1} fChOs (Fig. 4f). Only 3 of the 16 centrioles observed showed a normal 9-fold symmetrical arrangement of the microtubules, whilst the rest had symmetries ranging from 6-fold (n=5/16), 8-fold (n=6/16) to 10-fold (n=2/16). The defective symmetry extended from the basal body through the transition zone to the distal part of the cilium (Fig.4f). This phenotype is strikingly similar to defects in centriole symmetry of *Drosophila Sas6* mutants37.

Thus, loss of coordination in *gorab* mutants reflects the abnormal anatomy of the fChO resulting from absence of daughter centrioles and the abnormal symmetry of the remaining mother centriole-derived basal body.

Golgi and Centriole localisation domains of Gorab overlap

To address Gorab's functions at the centrosome and Golgi, we first wished to define domains responsible for its localisation to these sites. We began by defining the Gorab domain responsible for binding Sas6. We immobilised GST-tagged Sas6 on Glutathione Sepharose 4B beads and determined if it would bind ^{35}S-Met-labelled Gorab and or its fragments synthesised *in vitro* (Fig. 5a,b; Fig. S3a). We narrowed down strong binding of Sas6 to the 191-318 amino-acid interval of Gorab. The 244-338 amino-acid Gorab fragment also bound Sas6 but more weakly (Fig. S3a).Three non-overlapping smaller Gorab deletions (amino-acids 260-266, 267-281,and 282-286) also permitted Sas6 binding which was abolished by deletion of amino-acids 260-286, thus defining a Sas6-interacting-domain (SID) within this interval (Fig. 5c,d) To confirm that the *in vitro* interactions were reflected *in vivo*, we transiently transfected cultured *Drosophila* cells with myc-tagged Sas6 and either full-length GFP-Gorab or GFP-Gorab$^{\Delta SID}$(NP_788523.1:p.Cys260_Asn286). Western blots of GFP-pulldowns from cell extracts showed that Sas6 interacted with Gorab but not Gorab$^{\Delta SID}$ (Fig. S3b) confirming the *in vitro* binding results.

The SID domain lies within a predicted coiled-coil region (approximately amino-acids 190-320; Fig. 5e) in an analogous position to similar predicted domains of human GORAB (Fig. 5f). A previous study of human GORAB identified a fragment able to bind Arf5 and Rab6 in a yeast 2-hybrid system and in pull-down experiments; the IGRAB domain, amino-acids 99-27730. This same work identified a Golgi Targeting Domain (GTD) ofamino-acids 200-27730, corresponding to amino-acids 246-323in Drosophila Gorab. A missense mutation within the GTD, p.Ala220Pro occurring in gerodermia osteodysplastica patients, was found sufficient to disrupt Golgi localisation30,38. Sequence comparisons indicate *Drosophila* and human GORAB proteins are 70% similar and 40% identical in the GTD (Fig. 5g) and within *Drosophila* Gorab's putative GTD we could identify a conservative amino acid change to Valine at position 266 corresponding to Ala220 in the human GORAB sequence,. Thus, the parts of Gorab required for interactions with Sas6 and with the Golgi overlap; the site of the Golgi mislocalizing mutation lies within the Sas6-interacting-domain, which lies in turn within the putative GTD.

Gorab variants unable to localise to Golgi retain centriolar function

The overlapping nature of the SID with the potential site for Golgi localisation led us to ask whether mutations in this region would affect both functions. We asked whether the equivalent p.Val266Pro in *Drosophila* Gorab would disrupt its Golgi localization in the fly, and if so, how this might affect Gorab's centrosomal localisation and function. In addition we also generated transgenes having deletions corresponding to the SID (NP_788523.1:p.Cys260_Asn286), the putative GTD (NP_788523.1:p.Ala246_Ser323del), an N-terminal part of the GTD (N-GTD) (NP_788523.1: p.Ala246-Ala259del), and a C-terminal part (C-GTD) (NP_788523.1: p.Ala287_Ser323del) (Fig. 6a). We introduced these *gorab* variants into flies under the control of constitutive or inducible promoters and

integrated into the same genomic location using a site-specific integrase system allowing each to be expressed at a similar level (Online methods). An N-terminal eGFP tag on the mutant proteins allowed us to determine their subcellular localisation in larval imaginal disc cells. As above, the vast majority of wild-type eGFP-Gorab colocalized with Golgin245 in trans-Golgi and a small fraction was recruited to centrosomes. By contrast, Gorab mutants lacking the SID, the GTD and the N-terminal part of the GTD were diffusely distributed throughout the cytoplasm and did not accumulate at either Golgi or centrosomes (Fig. 6b). However, both the p.Val266Pro missense mutant and C-terminal GTD deletion retained their centrosomal localization despite losing their ability to localise to the Golgi (Fig. 6b).

To address whether centrosomally localized p.Val266Pro and ΔC-GTD mutant Gorab were still functional, we introduced transgenes expressing these Gorab mutant variants into a *gorab*^{1} null mutant background. This revealed that the *gorab*^{V266P} and *gorab*$^{\Delta C\text{-}GTD}$ transgenes could restore the climbing ability of *gorab*^{1} flies raised at 29 °C to a similar extent as *gorab*^{WT} whereas *gorab*$^{\Delta GTD}$, *gorab*$^{\Delta N\text{-}GTD}$ and *gorab*$^{\Delta SID}$ failed to do so (Fig. 6c). In addition, Gorab p.Val266Pro localized to the basal bodies in femoral chordotonal organs (Fig.S4). The female sterile phenotype of *gorab*^{1} was similarly rescued by *gorab*^{V266P} and *gorab*$^{\Delta C\text{-}GTD}$ but not by the other mutant transgenes (Fig. 6d). Thus, the centriole duplication defect of *gorab*^{1} is corrected by *gorab*^{V266P} and *gorab*$^{\Delta C\text{-}GTD}$. This separates the functions of Gorab showing that ability to localize to the centrosome and fulfil centriole duplication is distinct from any function of Gorab at the Golgi. By contrast, the ΔGTD, ΔN-GTD and ΔSID Gorab mutants could localize neither to the Golgi nor centrosomes and could not rescue the mutant phenotypes suggesting that they have completely lost both functions.

C-terminally tagged Gorab exerts Golgi dependent cytokinesis failure in the male germline

As golgins make functional interactions with Golgi membranes through their C-terminal sequences39, we attempted to disrupt the Golgi function of full-length Gorab by blocking its C-terminus. To this end we generated fly lines ubiquitously expressing C-terminally GFP-tagged Gorab. Males carrying a single copy of this *gorab*^{WT}*-GFP* transgene were sterile reflecting cytokinesis defects in male meiosis (Fig. 7a, b). Each wild-type spermatocyte undergoes meiosis to generate 4 haploid spermatids, each containing a mitochondrial derivative, the Nebenkern, visible as a phase-dense sphere of similar size to the haploid nucleus. By contrast, most *gorab*^{WT}*-GFP* spermatids had four nuclei and a single large Nebenkern indicative of cytokinesis failure (Fig. 7b). Immunostaining revealed C-terminally tagged Gorab formed string-like aggregates linking trans-Golgi compartments in mitotically dividing cells near the apex of the testes (Fig. 7c) and persisting into spermatocytes (Fig. 7d). In late anaphase, *gorab*^{WT}*-GFP*-expressing spermatocytes developed abnormal central spindles having irregularly shaped annilin rings with multiple protrusions that failed to constrict in telophase (Fig. 7d). These mutant spermatocytes strongly resembled those in COPI deficient flies40 leading us to hypothesise that expression of Gorab-GFP leads to Golgi associated defects.

We argued that if the C-terminal tag interfered with Gorab's Golgi function, then inclusion of either the p.Val266Pro or ΔSID mutations into a similar construct should relieve these

Golgi defects and restore male fertility. Indeed, transgenic flies expressing C-terminally GFP tagged p.Val266Pro and ΔSID mutant Gorab were fully fertile and showed no signs of cytokinesis failure (Fig. 7a, b). Interestingly, although *gorab*^{WT}*-GFP* resulted in cytokinesis defects in male germline, it was still able to rescue the coordination and female fertility defects of *gorab*^{1} mutants (Fig. S5). Thus, a C-terminal tag interferes with Gorab's Golgi function in meiotic spermatocytes without affecting its function at centrioles.

Discussion

Here we identify a tissue specific role for Golgi-associated Gorab in centriole duplication in *Drosophila.* Gorab physically interacts with the centriole cartwheel component, Sas6, with which it colocalises from the onset of procentriole formation. Centrosomes fail to duplicate in *gorab* mutant-derived embryos and in diploid tissues of *gorab* null *Drosophila*, which lose coordination through defects in their mechanosensory cilia. Such cilia have a single, mother centriole-derived basal body with between 6 to 10 sets of microtubules, the abnormal symmetry extending into the ciliary axoneme.

Loss of 9-fold symmetry in *gorab* mutant centrioles is reminiscent of *Sas6* mutants37. It suggests the Gorab- Sas6 partnership is required for both centriole duplication and symmetry. The formation of centrioles with correct symmetry can still be directed around Sas6 variants that are themselves unable to establish9-fold symmetry24,25. This suggests other components of the centriole, in addition to Sas6, also contribute to its symmetry. Gorab could be one such contributing molecule, at least in part. However, this cannot be universally true because centrioles and axonemes in the gonads of fully fertile *gorab* null males have correct9-fold symmetry (not shown). This could be either because maternal Gorab protein perdures sufficiently in male germ cells to permit centriole duplication or because Gorab is substituted by another molecule in spermatogenesis. These possibilities, either of which could reflect the distinctive morphology of *Drosophila's* spermatocyte centrioles, require further study.

The trans-Golgi localization of human GORAB30 is mirrored in multiple *Drosophila* tissues including salivary glands, imaginal discs, the central nervous system, and in the male and female germ lines but not in syncytial embryos, where Golgi has yet to form. Accordingly, Gorab's association with COPI coatomer components in cultured cells suggests involvement in retrograde vesicle transport from Golgi to ER consistent with its resemblance to a golgin. The rod-like golgins, which bind Rab, Arf, or ADP-ribosylation family GTPases, are tethered to Golgi membranes by their C-termini and protrude outwards to capture vesicles at their N-termini39. Overlapping specificity in vesicle targeting provides redundancy of function. Thus, both golgins GMAP-210 and GM130 can capture ER-derived carriers; both GMAP-210 and Golgin-84 can capture cis-Golgi derived vesicles; and so on41. Such redundancy might account for the lack of any Golgi phenotype in *gorab* null mutants. However, Gorab's functional relevance at the *Drosophila* Golgi is indicated by the cytokinesis defects in male meiosis caused by expression ofC-terminally tagged Gorab, which are strikingly similar to those following disruption of COPI-mediated vesicle trafficking40. This accords with Gorab's association with COPI proteins and reinforces

suggestions that integrity of ER and other membraneous structures is interdependent with astral and spindle microtubule function in male meiosis.

By generating the counterpart of a gerodermia osteodysplastica missense mutant that prevents human GORAB from localising to Golgi30, we can separate *Drosophila* Gorab's Golgi and centriole functions. Thisp.Val266Pro mutation prevents Gorab from associating with Golgi but fully rescues centriole duplication defects of *gorab* null mutants and restores their ciliary function. A proline residue at this site could strongly influence structure of the Golgi-interacting region because of its side chain's rigidity and ability to undergo cis-trans isomerisation. The mutation does not, however, interfere with Gorab's ability to bind Sas6. Moreover, introducing p.Val266Pro into C-terminally tagged Gorab prevents its localization to Golgi and so relieves the cytokinesis defect. Thus the male sterility resulting from a C-terminal GFP tag is mediated through Gorab's Golgi association. Gorab's precise Golgi functions in *Drosophila,* most likely redundant with other golgins, must await further genetic and molecular studies.

Gorab is not required for centriole duplication or Golgi function in unicellular organisms such as ciliated eukaryotes. Its evolutionary appearance in metazoans may reflect increased proximity and functional interactions between the Golgi, centrosomes and cilia (see Introduction). Such co-evolution could have facilitated the emergence of proteins with dual functions allowing a component of one organelle to "moonlight" in its neighbor. However, Gorab is not present in all metaozoans; it is absent, for example, from *C.elegans*. This could possibly reflect the assembly of *C. elegans* SAS6 into a spiral rather than the ring-shaped oligomers characteristic of the centriole cartwheels in most species42, which may obviate the need for interactions with a Gorab-like protein. Moreover, even within a single species, Gorab may be required for centriole duplication in some tissues and not others, as we find in *Drosophila*. Such tissue specificity might account for findings with a *GORAB* mutant mouse, which has few primary cilia in dermal condensate cells responsible for Hedgehog signaling in hair follicles but does have primary cilia on keratinocytes43. This could reflect tissue specific failure of centriole duplication in the null mouse even though there is currently no evidence to support this notion.

Although the above defects in cilia development in the *GORAB* null mouse require molecular analysis, they suggest a possibility of conserved roles for GORAB. Both fly and human proteins are not only found at the trans-Golgi (this study;30) but also at the centriole (Figs. 1,2; Fig. S6a,b). We expressed GFP-tagged GORAB in U2OS cells and found it at both centrosomes and Golgi. The Golgi localization was abolished by the p.Ala220Pro mutation but centrosome association remained (Fig S6a). We also found anti-GORAB antibodies could detect human GORAB at the centriole albeit not always together with Sas6 as in *Drosophila*(Fig. S6b). This might reflect different requirements for GORAB and Sas6 at the centriole in the two organisms; Sas6 remains centriole associated throughout the *Drosophila* duplication cycle whereas it is first recruited and then is later absent from the lumen of the mother centriole for a substantial part of the human duplication cycle44,45. It will be of future interest to track the precise behaviors of SASS6 and GORAB throughout the centriole duplication cycle in human cells.

Currently, however, it remains uncertain whether GORAB functions in centriole duplication in human cells as in insects (Fig. S6). Because mammalian cells lacking centrosomes are prevented from cell cycle progression by a p53 dependent pathway25,46,47, we attempted to assess the consequences of GORAB depletion upon centrosome number in a human osteosarcoma (U2OS) line expressing dominant negative p53 (U2OS p53DD)48. In our experience, some more stable centriole proteins require more rounds of knockdown before a duplication phenotype can be observed and, unfortunately, GORAB RNAi led to cell death before depletion was complete. This was possibly due to compromised Golgi function, making it difficult to assess the effect upon centriole duplication. However, GORAB RNAi enhanced the centrosome loss seen following depletion of SASS6 alone suggesting the possibility of a co-operative role between the two proteins (Fig. S6c). We also found that depletion of human GORAB abolished the centrosome overduplication that occurs in U2OScells held in S-phase following Aphidicolin and Hydroxyurea treatment (Fig. S6d,e). However, because Golgi function is also compromised by these treatments, we cannot be certain that human GORAB is required for centrosome duplication as in flies.

We note that thep.Ala220Pro mutation results in a comparable disease phenotype to null mutations26,38. As GORAB p.Ala220Pro can still associate with the centrosome, this suggests the gerodermia osteodysplastica phenotype is likely to result predominantly from defective Golgi functioning. However, it remains of future interest to re-examine cells from different tissues of patients with GORAB null mutations for potential additional defects in centriole duplication and/or formation of primary cilia. It will also be important to examine GORAB -/- mice further to determine whether the reported loss of cilia could arise through failure of centriole duplication rather than a secondary consequence of Golgi malfunction.

To conclude, our findings bring insight into the dual life of a protein with Golgi and centriole functions but also raise new future questions. An understanding of the precise role of Gorab at the Golgi awaits a greater knowledge of Gorab’s Golgi partners and redundancy with other golgins. Moreover, full understanding of Gorab’s centriole duplication function in *Drosophila* awaits future studies of its precise structural interactions with Sas6 and other centriole proteins.

Online Methods

In vivo ProteinA and GFP-trap purification from Drosophila cells and embryos for mass spectrometry

To identify protein complexes in vivo, a combination of single step ProteinA affinity or GFP trap purification and Mass Spectrometry was performed as previously described49,50.

In vitro binding assay

In vitro binding assays between ^{35}S-Methionine-labelled proteins produced by coupled transcription and translation *in vitro and* GTS-tagged bacterially expressed protein immobilised on resin were carried out as described5.

Structured illumination microscopy

Structured illumination microscopy of D.Mel-2 cells was carried out as described in 51. For 3D-SIM in human U-2 OS cell, cells were fixed in ice-cold methanol, washed with PBST and blocked in PBST containing 10%FCS for 30 min. The following primary antibodies were used diluted in PBST containing 10%FCS: rabbit anti-Gorab (1:200, Atlas, #HPA027250, specificity also tested in this study, fig. S6f,g), rabbit anti-Pericentrin (1:200, Abcam,#ab4448, directly labeled with Alexa594), mouse monoclonal anti-Sas6 (1:100, Santa-Cruz Biotechnology, #sc-81431). An OMX-V3 system was used with a 63x/1.4NA oil Olympus lens to acquire super-resolution images (512x512ppi). Images were reconstructed and registered using the SoftWorx Linux package and processed to obtain maximum intensity projections.

Fly stocks

Gorab deletion null mutants were generated using an optimized CRISPR/Cas9 mutagenesis tool for Drosophila genome engineering52. All guide RNAs were cloned into pCFD3 (guide RNA expressing vector Addgene, Cat. No. 49410). Transgenic flies were generated using site-specific transformation via φC31 integrase-mediated cassette exchange53,54. Guide RNAs targeting the 5' end of *gorab* were integrated on the 2nd chromosomal attP40 landing site, whilst internal and 3' end guide RNAs were integrated on the 3rd chromosomal attP2 landing site. Afterwards, 5' and 3' end targeting guide RNA transformants were combined in crosses. The guide RNA-mediated double strand breaks were induced by crossing these flies to a strain expressing Cas9 via a germline specific *nanos* promoter (*nos-Cas9*, Bloomington ID: 54591). The emerged G_0 (cut starter) flies were individually crossed to third chromosomal balancer lines. In total, 215 mutant candidates from the next generation were subjected to PCR. We identified two deletion alleles, $gorab^1$(NT_037436.4:g.33_507del)and $gorab^2$(NT_037436.4:g.1_1097del), and their precise breakpoints were determined by sequencing. Primers used for mutagenesis experiment are described in Supplementary Table S3.

For the rescue and localization studies, all transgenes were integrated into the same, attP2 landing site to achieve the same level of expression. In order to make the pPGW, pUGW and pUWG Drosophila Gateway™ (Thermo Fisher Scientific) destination vectors able to integrate into attP sites by φC31 mediated recombination, we integrated an attB site into these vectors. First, a 275 bp sequence containing the 51 bp core *Streptomyces lividans* attB recombination site was amplified by PCR from pUASTattB54. The PCR product was than blunted and ligated into the AfeI site of pPGW, pUGW and pUWG vectors. The AfeI site in these vectors is a single cutter site and does not affect any functional components of the vectors. The integration and orientation of the attB site was verified by sequencing. Gateway™(Thermo Fisher Scientific) compatible *gorab* entry clone was generated by amplifying the *gorab* coding seqeunce from the RE68977 cDNA clone (Drosophila Genomics Resource Center) and introduced into pDONR221 entry vector by a BP reaction. Wild type and *gorab* mutant coding sequences generated by site-directed mutagenesis were recombined by Gateway™ LR recombination into pPGWattB and pUGWattB vectors. The resulting transgenes were injected into flies carrying the attP2 landing site and expressing φC31 integrase. Although the LR reaction generates two shorter attB sites (attB1 and attB2),

our experience is that these sites are not interfering with the appropriate integration of the constructs via the attB site we included at the AfeI site. In fact, every transformant of 19 different transgenic constructs expressed the transgene properly, as tested by immunofluorescence and western blot.

The pUASp-GFP-Root transgenic fly line was kindly provided by Timothy L. Megraw. The Ubq-YFP-Centrobin transgenic fly line was obtained from Cayetano Gonzalez.

An Oregon-R stock was used as wild type control. All flies in the described experiments were maintained on standard Drosophila medium and at 25 °C unless otherwise indicated.

Detailed genotypes of fly stocks used in this study:

y M{w^{+mC}=nos-Cas9.P}ZH-2A w (Chr X, BDSC 54591; Cas9 source for *gorab* mutagenesis)

w; gorab^{1}/ TM6B, Tb Hu (Chr 3, this study)

w; gorab^{2}/ TM6B, Tb Hu (Chr 3, this study)

P{w$^{+mC.hs}$=GawB}elav^{C155} (Chr X, BDSC 458; driver line used for neuronal expression)

y w P{y$^{+t7.7}$=nos-phiC31\int.NLS}X #12;P{y$^{+t7.7}$=CaryP}attP2 (Chr X and 3, BDSC 25710; landing site used for all *gorab* transgenes)

w; pUASp-GFP-Root (Chr 2, from Timothy L. Megraw)

w; pWR-Ubq-YFP-Cnb (Chr 2, from Cayetano Gonzalez)

Fertility test

To test the fertility of wild type, *gorab* mutant and transgenic females, virgin females were collected and individually mated with two Oregon-R males (age 2-4 days). The crosses were kept at 25 °C for 6 days and the adults then removed. The numbers of eclosed progeny in each vial were recorded and statistically analysed. Vials in which any adults died, were not considered. 15 crosses were evaluated per genotype. To test the fertility of wild type, *gorab* mutant and transgenic males, 1-2 days old males were crossed to individual Oregon-R virgin females (aged 4 days before mating, to test their virginity). The crosses were kept at 25 °C for 6 days before adults were then removed. The numbers of eclosed progeny in each vial were recorded and statistically analyzed. Vials in which any of the adults died, were not considered. 15 crosses were evaluated per genotype.

Testing coordination

To quantitatively evaluate coordination, wild type, *gorab* mutant and transgenic flies were raised at 29°C. This temperature was chosen as it accentuates the uncoordinated phenotype of *gorab^{1}*. Pupae grown at this temperature were removed from their original vial and transferred into a vial without media to prevent the uncoordinated flies from sticking to the media. The day before the experiments, cohorts of 15 flies were transferred into fresh vials with media. Immediately before the assay, flies were transferred without anaesthesia into a

clear empty testing vial. For the assay, vials were illuminated from above, flies gently tapped down to the bottom of the vial, and then given 1 min to climb up the vial. Numbers of flies crossing the 5 cm mark were then recorded. The climbing assay was repeated three times for each cohort with similar results. 3 independent cohorts of 15 flies were tested per genotype.

For startle response experiments, flies raised at 29 °C were placed into empty 3cm diameter plastic Petri dishes, which were gently shaken 3 to 5 times sideways (the startle). 30 sec long videos were then captured to demonstrate the state of coordination of the flies after the startle.

Transmission electron microscopy

Cross- and longitudinal sections of antenna of flies was fixed and imaged as described in 36.

RNA interference in cultured cells

Human bone osteosarcoma epithelial U-2 OS and U-2 OS^{p53DD}cells were cultured, transfected and analyzed as described in 55. U-2 OS were stated mycoplasma free upon receive by were not tested by authors for mycoplasma contamination. Combination of three different Silencer Select siRNAs for Gorab (Thermo Fisher Scientific, #s40927, s40928, s40929) and Sas-6 (Thermo Fisher Scientific, #s225787, s46485, s46486) were used with Lipofectamine RNAi Max (Thermos Fisher Scientific) to achieve efficient knockdown.

Antibody generation

Two polyclonal antibodies were generated against the respective N- (1-169 amino acids) and C- (177-338) terminal parts of the Drosophila Gorab protein. His-tagged N- and C-terminal Gorab fragments were expressed in DH5α E.coli bacterial strain under the control of T7 promoter by induction with 1 mM IPTG for 4 h at 37 °C. The proteins were purified on a Ni-NTA column (Qiagen) with standard urea containing buffers according to the manufacturer's instructions. The purified proteins were used to immunise Guinea pigs by Moravian Biotech according to standard protocols. The specificities of the purified antibodies were tested on wild type and *gorab* silenced D.Mel-2 cell lines by immunostaining (fig. S1d) and in *gorab* null mutant flies by western blot (Fig.3c). A dilution of 1:5000 was used for western blots and 1:500 for immunostaning experiments.

Immunohistochemistry and confocal microscopy

For immunostaining of D.Mel-2 cells, cells were fixed either with chilled methanol (when staining for centrosome markers) or 4% formaldehyde, for 30 min. After fixation, cells were washed in PBS containing 0.1% TritonX100 (PBST) for 5 min, followed by blocking in PBST containing 10% FCS for 30 min. The following primary antibodies were used following dilution in PBST containing 10%FCS: chicken anti-dPLP (1:1000, ref.37), rat anti-Sas6 (1:1000, ref.5), guinea pig anti-Gorab(1:1000, this study), goat anti-Golgin245 (1:500, ref.56, provided by Sean Munro), rabbit anti-GM130 (1:500, Abcam, #ab30637). After 1h incubation, cells were washed 3 times for 5 min with PBST, followed by a 1h incubation with appropriate secondary antibodies diluted 1:300 in PBST containing 10%FCS. After three 5 min PBST washes, cells were mounted in Vectashield containing DAPI.

To immunostain human cell lines (U-2 OS and U-2 OS^{p53DD}) for centrosome counting, cells were fixed in ice-cold methanol, washed with PBST and blocked in PBST containing 10%FCS for 30 min. The following primary antibodies were used diluted in PBST containing 10%FCS: mouse anti-gamma-tubulin (1:200, Sigma, #T6557, clone GTU-88, ascites fluid), rabbit anti-CENP-J (1:200, Abcam, #ab221134). After 1h incubation, cells were washed 3 times for 5 min with PBST, followed by a 1h incubation with appropriate secondary antibodies diluted 1:300 in PBST containing 10%FCS. After three 5 min PBST washes, cells were mounted in Vectashield containing DAPI.

To immunostain U-2 OS cells transiently expressing *GFP-Gorab*^{wt} or *GFP-Gorab*^{A220P}, cells were fixed in 4% formaldehyde for 20 min to preserve the Golgi structures. After fixation, cells were washed with PBST and blocked in PBST containing 10%FCS for 1 hour. The following primary antibodies were used following dilution in PBST containing 10%FCS: rabbit anti-Pericentrin (1:4000, Abcam, #ab4448), mouse anti-Golgin 97 (1:200, Abcam, #ab169287). After 1h incubation, cells were washed 3 times for 5 min with PBST, followed by a 1h incubation with appropriate secondary antibodies diluted 1:300 in PBST containing 10%FCS. After three 5 min PBST washes, cells were mounted in Vectashield containing DAPI.

For the immunostaning of syncytial Drosophila embryos, 0-2h synchronized embryos were dechorionated and fixed in 4% formaldehyde for 30 min. Following a 30 min wash in PBS, embryos were manually devitellinised, permeabilized for 30 min in PBST, and then incubated in PBST containing 10% FCS for 1h to block the fixative. Embryos were then incubated overnight at 4 °C in following primary antibodies: mouse anti-α-tubulin (1:200, Abcam, ab7291), rabbit anti-CNN (1:200, ref.57), rabbit anti-asterless (1:400, ref.58), goat anti-Golgin245 (1:100). After three 20 min PBST washes, the appropriate secondary antibodies were applied for 4h at room temperature. After three 20 min PBST washes, embryos were mounted in Vectashield+DAPI.

Larval brains and imaginal discs were dissected from third instar wandering larvae and fixed in 4% formaldehyde for 30 min, followed by three 20 min PBST washes. Staining was then carried out as above. The following primary antibodies were used: chicken anti-dPLP (1:200), goat anti-Golgin245 (1:200). The same protocol was applied for testis preparations stained for dPLP and Golgin245. Testes were stained with antibodies against α-tubulin and anillin as described in 59.

To immuno-stain femoral chordotonal organ (fChO), flies were raised at 29 °C until the pharate adult stage. The pupal case was removed in PBS and whole pharate adults were fixed in 4% formaldehyde for 30 min, followed by washes in PBST. The fine dissection of fixed legs was performed in PBS using superfine edged Dumon 5SF tweezers. The part of the femur containing the fChO was cut out and the cuticle opened up to facilitate penetration of the antibodies. The immunostaining was then performed as with larval brains and imaginal discs.

All microscopic preparations were imaged using a Leica SP8 confocal laser scanning microscope and processed with ImageJ.

Statistics

For female and male fertility tests and for climbing assays we estimated the sample size based on literature60,61 except that we increased the sample size from at n= 6 individuals per genotype used by Zhong and Belote to n=15 individual flies thus increasing the statistical power and reduce the standard deviation. All fertility tests were independently repeated once with n=15 individual flies. In the climbing assay, Chen et al used 10 individuals per genotype whereas we increased the sample size to 15 individuals. The experiments were done in three independent replicates, n=15 individual flies in each replica. The indistinguishable appearance of Drosophila individuals of the same genotype ensures that the flies were blindly and randomly collected for fertility and coordination tests. Flies dying during the assays were excluded from analysis and the test was repeated. For counting centrosomes in human cell lines, replicates consist of cells independently treated with siRNA/Aphidicoline+Hydroxyurea as indicated in figure legends. Each treated replica was mounted and imunostained on an idependent coverslip. Centrosomes in randomly selected cells (n=100) were counted in each replica. Number of replicates (N), mean and standard error of mean (s.e.m) are indicated in corresponding figure legends. Online Shapiro-Wilk test (http://sdittami.altervista.org/shapirotest/ShapiroTest.html)was used to test for normal distribution. Data collected from coordination assays, fertility tests and centrosomes counts were analyzed with two-tailed unpaired t-testinitially in Microsoft Office Excel (version 2007) and subsequently verified by GraphPad Prism (version 5.01)p values for each analysis are indicated in corresponding figure legends. 99% confidence interval was applied in all statistical tests.

Supplementary Material

Refer to Web version on PubMed Central for supplementary material.

Acknowledgments

DMG is grateful for a Wellcome Investigator Award which supported this work. The study was initiated with support from Cancer Research UK. We would like to acknowledge Péter Deák for his encouragement and support of LK and Margit Pál for injection of CRISPR/Cas9 guide RNAs for Gorab mutagenesis, Sang Chang, Kadri Oras and Alla Madich for injection of Gorab transgenes. We also greatly appreciate the advice of Magdalena Richter and Agnieszka Fatalska in studies of protein-protein interactions. We thank Tim Megraw (Department of Biomedical Sciences, Florida State University, Tallahassee, FL, USA)for GFP-Rootletin flies, Cayetano Gonzalez (Institute for Research in Biomedicine, The Barcelona Institute of Science and Technology, Barcelona, Spain) for YFP-Centrobin flies, Sean Munro (MRC Laboratory of Molecular Biology, Cambridge, UK) for anti-Golgin antibodies, Ken Raj (Radiation Effects Department, Public Health England, Didcot, UK) for U-2 OS^{p53DD} cell line and Janusz Debski for advice in mass-spectrometry.

References

1. Gönczy P. Towards a molecular architecture of centriole assembly. Nature Reviews Molecular Cell Biology. 2012; 13:425–435. [PubMed: 22691849]
2. Goshima G, et al. Genes Required for Mitotic Spindle Assembly in Drosophila S2 Cells. Science. 2007; 316:417–421. [PubMed: 17412918]
3. Dobbelaere J, et al. A Genome-Wide RNAi Screen to Dissect Centriole Duplication and Centrosome Maturation in Drosophila. PLoS Biology. 2008; 6:e224. [PubMed: 18798690]

4. Dzhindzhev NS, et al. Two-step phosphorylation of Ana2 by Plk4 is required for the sequential loading of Ana2 and Sas6 to initiate procentriole formation. Open Biology. 2017; 7:170247. [PubMed: 29263250]
5. Dzhindzhev NS, et al. Plk4 phosphorylates Ana2 to trigger Sas6 recruitment and procentriole formation. Curr Biol. 2014; 24:2526–2532. [PubMed: 25264260]
6. Ohta M, et al. Direct interaction of Plk4 with STIL ensures formation of a single procentriole per parental centriole. Nature Communications. 2014; 5:5267.
7. Hiraki M, Nakazawa Y, Kamiya R, Hirono M. Bld10p Constitutes the Cartwheel-Spoke Tip and Stabilizes the 9-Fold Symmetry of the Centriole. Current Biology. 2007; 17:1778–1783. [PubMed: 17900905]
8. Jerka-Dziadosz M, et al. Basal body duplication in Paramecium: The key role of Bld10 in assembly and stability of the cartwheel. Cytoskeleton. 2010; NA-NA. doi: 10.1002/cm.20433
9. Lin Y-C, et al. Human microcephaly protein CEP135 binds to hSAS-6 and CPAP, and is required for centriole assembly. EMBO J. 2013; 32:1141–1154. [PubMed: 23511974]
10. Tang C-JC, Fu R-H, Wu K-S, Hsu W-B, Tang TK. CPAP is a cell-cycle regulated protein that controls centriole length. Nature Cell Biology. 2009; 11:825–831. [PubMed: 19503075]
11. Schmidt TI, et al. Control of Centriole Length by CPAP and CP110. Current Biology. 2009; 19:1005–1011. [PubMed: 19481458]
12. Kohlmaier G, et al. Overly Long Centrioles and Defective Cell Division upon Excess of the SAS-4-Related Protein CPAP. Current Biology. 2009; 19:1012–1018. [PubMed: 19481460]
13. Wang W-J, Soni RK, Uryu K, Bryan Tsou M-F. The conversion of centrioles to centrosomes: essential coupling of duplication with segregation. The Journal of Cell Biology. 2011; 193:727–739. [PubMed: 21576395]
14. Izquierdo D, Wang W-J, Uryu K, Tsou M-FB. Stabilization of Cartwheel-less Centrioles for Duplication Requires CEP295-Mediated Centriole-to-Centrosome Conversion. Cell Reports. 2014; 8:957–965. [PubMed: 25131205]
15. Fu J, et al. Conserved molecular interactions in centriole-to-centrosome conversion. Nat Cell Biol. 2016; 18:87–99. [PubMed: 26595382]
16. Efimov A, et al. Asymmetric CLASP-dependent nucleation of noncentrosomal microtubules at the trans-Golgi network. Dev Cell. 2007; 12:917–930. [PubMed: 17543864]
17. Rivero S, Cardenas J, Bornens M, Rios RM. Microtubule nucleation at the cis-side of the Golgi apparatus requires AKAP450 and GM130. EMBO J. 2009; 28:1016–1028. [PubMed: 19242490]
18. Rios RM. The centrosome-Golgi apparatus nexus. Philos Trans R Soc Lond B Biol Sci. 2014; 369
19. Emmer BT, Maric D, Engman DM. Molecular mechanisms of protein and lipid targeting to ciliary membranes. Journal of Cell Science. 2010; 123:529–536. [PubMed: 20145001]
20. Kim H, et al. Ciliary membrane proteins traffic through the Golgi via a Rabep1/GGA1/Arl3-dependent mechanism. Nature Communications. 2014; 5:5482.
21. Stoetzel C, et al. A mutation in VPS15 (PIK3R4) causes a ciliopathy and affects IFT20 release from the cis-Golgi. Nature Communications. 2016; 7:13586.
22. Follit JA, et al. The Golgin GMAP210/TRIP11 anchors IFT20 to the Golgi complex. PLoS Genet. 2008; 4:e1000315. [PubMed: 19112494]
23. Broekhuis JR, Rademakers S, Burghoorn J, Jansen G. SQL-1, homologue of the Golgi protein GMAP210, modulates intraflagellar transport in C. elegans. J Cell Sci. 2013; 126:1785–1795. [PubMed: 23444385]
24. Hilbert M, et al. SAS-6 engineering reveals interdependence between cartwheel and microtubules in determining centriole architecture. Nat Cell Biol. 2016; 18:393–403. [PubMed: 26999736]
25. Wang W-J, et al. De novo centriole formation in human cells is error-prone and does not require SAS-6 self-assembly. Elife. 2015; 4
26. Hennies HC, et al. Gerodermia osteodysplastica is caused by mutations in SCYL1BP1, a Rab-6 interacting golgin. Nature Genetics. 2008; 40:1410–1412. [PubMed: 18997784]
27. Di Y, et al. Cloning and characterization of a novel gene which encodes a protein interacting with the mitosis-associated kinase-like protein NTKL. J Hum Genet. 2003; 48:315–321. [PubMed: 12783284]

28. Burman JL, et al. Scyl1, mutated in a recessive form of spinocerebellar neurodegeneration, regulates COPI-mediated retrograde traffic. J Biol Chem. 2008; 283:22774–22786. [PubMed: 18556652]
29. Burman JL, Hamlin JNR, McPherson PS. Scyl1 regulates Golgi morphology. PLoS ONE. 2010; 5:e9537. [PubMed: 20209057]
30. Egerer J, et al. GORAB Missense Mutations Disrupt RAB6 and ARF5 Binding and Golgi Targeting. J Invest Dermatol. 2015; 135:2368–2376. [PubMed: 26000619]
31. Ripoche J, Link B, Yucel JK, Tokuyasu K, Malhotra V. Location of Golgi membranes with reference to dividing nuclei in syncytial Drosophila embryos. Proc Natl Acad Sci USA. 1994; 91:1878–1882. [PubMed: 8127899]
32. Papoulas O, Hays TS, Sisson JC. The golgin Lava lamp mediates dynein-based Golgi movements during Drosophila cellularization. Nat Cell Biol. 2005; 7:612–618. [PubMed: 15908943]
33. Frescas D, Mavrakis M, Lorenz H, Delotto R, Lippincott-Schwartz J. The secretory membrane system in the Drosophila syncytial blastoderm embryo exists as functionally compartmentalized units around individual nuclei. J Cell Biol. 2006; 173:219–230. [PubMed: 16636144]
34. Basto R, et al. Flies without centrioles. Cell. 2006; 125:1375–1386. [PubMed: 16814722]
35. Blachon S, et al. A proximal centriole-like structure is present in Drosophila spermatids and can serve as a model to study centriole duplication. Genetics. 2009; 182:133–144. [PubMed: 19293139]
36. Gottardo M, et al. Loss of Centrobin Enables Daughter Centrioles to Form Sensory Cilia in Drosophila. Curr Biol. 2015; 25:2319–2324. [PubMed: 26299513]
37. Rodrigues-Martins A, et al. DSAS-6 organizes a tube-like centriole precursor, and its absence suggests modularity in centriole assembly. Curr Biol. 2007; 17:1465–1472. [PubMed: 17689959]
38. Al-Dosari M, Alkuraya FS. A novel missense mutation in SCYL1BP1 produces geroderma osteodysplastica phenotype indistinguishable from that caused by nullimorphic mutations. Am J Med Genet A. 2009; 149A:2093–2098. [PubMed: 19681135]
39. Gillingham AK, Munro S. Finding the Golgi: Golgin Coiled-Coil Proteins Show the Way. Trends in Cell Biology. 2016; 26:399–408. [PubMed: 26972448]
40. Kitazawa D, Yamaguchi M, Mori H, Inoue YH. COPI-mediated membrane trafficking is required for cytokinesis in Drosophila male meiotic divisions. J Cell Sci. 2012; 125:3649–3660. [PubMed: 22553212]
41. Wong M, Munro S. The specificity of vesicle traffic to the Golgi is encoded in the golgin coiled-coil proteins. Science. 2014; 346:1256898–1256898. [PubMed: 25359980]
42. Hilbert M, et al. Caenorhabditis elegans centriolar protein SAS-6 forms a spiral that is consistent with imparting a ninefold symmetry. Proc Natl Acad Sci USA. 2013; 110:11373–11378. [PubMed: 23798409]
43. Liu Y, et al. Gorab Is Required for Dermal Condensate Cells to Respond to Hedgehog Signals during Hair Follicle Morphogenesis. J Invest Dermatol. 2016; 136:378–386. [PubMed: 26967474]
44. Strnad P, et al. Regulated HsSAS-6 levels ensure formation of a single procentriole per centriole during the centrosome duplication cycle. Dev Cell. 2007; 13:203–213. [PubMed: 17681132]
45. Fong CS, Kim M, Yang TT, Liao J-C, Tsou M-FB. SAS-6 assembly templated by the lumen of cartwheel-less centrioles precedes centriole duplication. Dev Cell. 2014; 30:238–245. [PubMed: 25017693]
46. Lambrus BG, et al. p53 protects against genome instability following centriole duplication failure. The Journal of Cell Biology. 2015; 210:63–77. [PubMed: 26150389]
47. Lambrus BG, et al. A USP28–53BP1–p53–p21 signaling axis arrests growth after centrosome loss or prolonged mitosis. The Journal of Cell Biology. 2016; 214:143–153. [PubMed: 27432896]
48. Raj K, Ogston P, Beard P. Virus-mediated killing of cells that lack p53 activity. Nature. 2001; 412:914–917. [PubMed: 11528480]
49. D'Avino PP, et al. Isolation of protein complexes involved in mitosis and cytokinesis from Drosophila cultured cells. Methods Mol Biol. 2009; 545:99–112. [PubMed: 19475384]
50. Lipinszki Z, et al. Affinity purification of protein complexes from Drosophila embryos in cell cycle studies. Methods Mol Biol. 2014; 1170:571–588. [PubMed: 24906338]

51. Fu J, Glover DM. Structured illumination of the interface between centriole and peri-centriolar material. Open Biol. 2012; 2:120104. [PubMed: 22977736]
52. Port F, Chen H-M, Lee T, Bullock SL. Optimized CRISPR/Cas tools for efficient germline and somatic genome engineering in Drosophila. Proc Natl Acad Sci USA. 2014; 111:E2967–2976. [PubMed: 25002478]
53. Groth AC, Fish M, Nusse R, Calos MP. Construction of transgenic Drosophila by using the site-specific integrase from phage phiC31. Genetics. 2004; 166:1775–1782. [PubMed: 15126397]
54. Bischof J, Maeda RK, Hediger M, Karch F, Basler K. An optimized transgenesis system for Drosophila using germ-line-specific phiC31 integrases. Proc Natl Acad Sci USA. 2007; 104:3312–3317. [PubMed: 17360644]
55. Fu J, et al. Conserved molecular interactions in centriole-to-centrosome conversion. Nat Cell Biol. 2016; 18:87–99. [PubMed: 26595382]
56. Riedel F, Gillingham AK, Rosa-Ferreira C, Galindo A, Munro S. An antibody toolkit for the study of membrane traffic in Drosophila melanogaster. Biol Open. 2016; 5:987–992. [PubMed: 27256406]
57. Heuer JG, Li K, Kaufman TC. The Drosophila homeotic target gene centrosomin (cnn) encodes a novel centrosomal protein with leucine zippers and maps to a genomic region required for midgut morphogenesis. Development. 1995; 121:3861–3876. [PubMed: 8582295]
58. Dzhindzhev NS, et al. Asterless is a scaffold for the onset of centriole assembly. Nature. 2010; 467:714–718. [PubMed: 20852615]
59. Sechi S, et al. Rab1 interacts with GOLPH3 and controls Golgi structure and contractile ring constriction during cytokinesis in Drosophila melanogaster. Open Biol. 2017; 7
60. Zhong L, Belote JM. The testis-specific proteasome subunit Pros 6T of D. melanogaster is required for individualization and nuclear maturation during spermatogenesis. Development. 2007; 134:3517–3525. [PubMed: 17728345]
61. Chen JV, et al. Rootletin organizes the ciliary rootlet to achieve neuron sensory function in Drosophila. The Journal of Cell Biology. 2015; 211:435–453. [PubMed: 26483560]

Europe PMC Funders Author Manuscripts

Europe PMC Funders Author Manuscripts

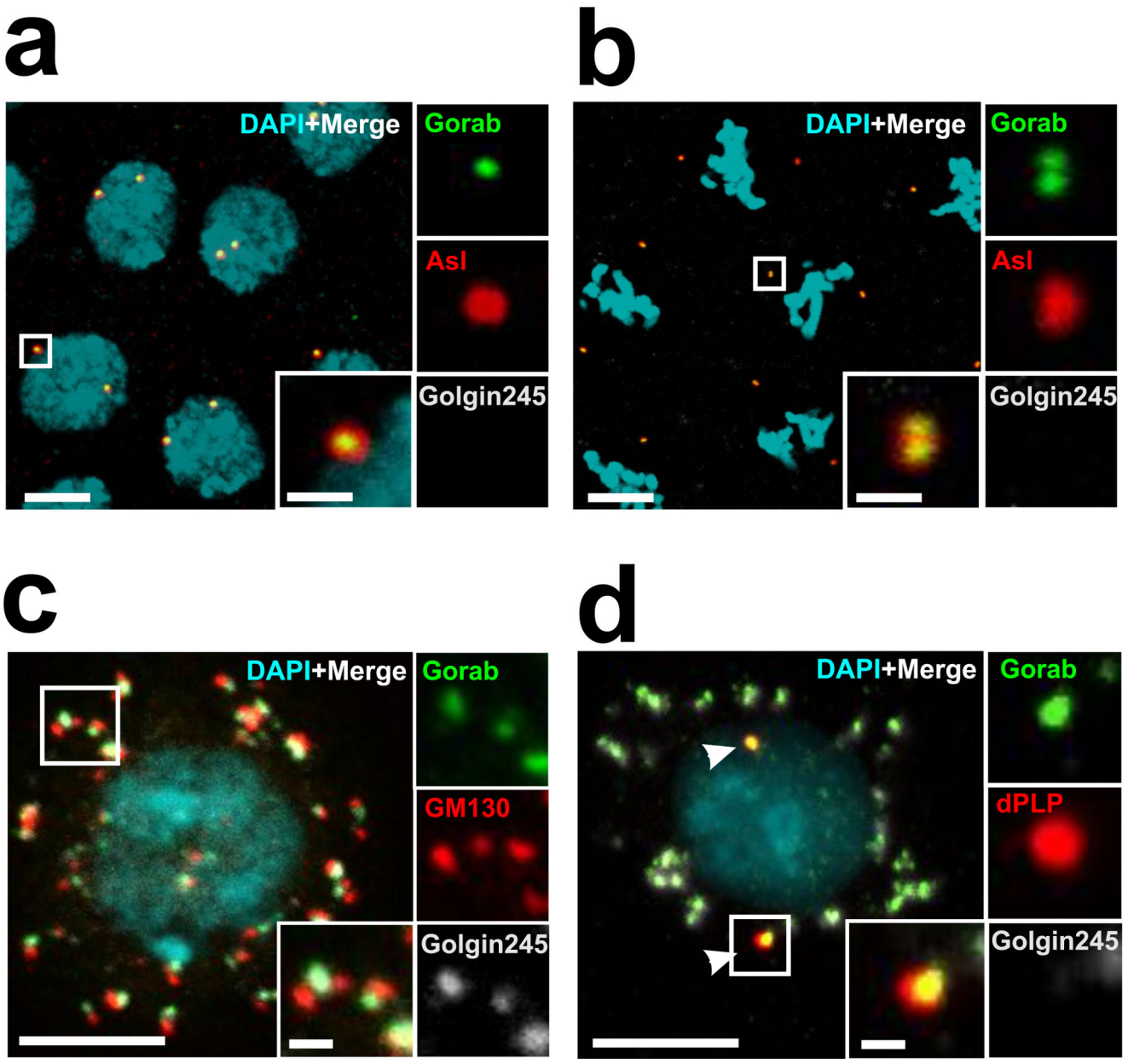

Fig. 1. Gorab associates with both Centrosomes and Golgi

(**a,b**) Syncytial embryos expressing poly-Ubiquitin-GFP-Gorab and stained to reveal Asterless (Asl) and the trans-Golgi Golgin245 in a field of interphase (**a**) and mitotic (**b**) nuclei. Experiments repeated 3 times with similar results. Main scale bar, 5 μm; Inset scale bar, 1 μm(**c**) Cultured D.Mel-2 cells immuno-stained to reveal Gorab, GM130 (cis-Golgi), and Golgin245 (trans-Golgi).Experiment repeated 3 times with similar results. Main scale bar, 5 μm; Inset scale bar, 0.5 μm.(**d**) Cultured D.Mel-2 cells immunostained to reveal Gorab, dPLP (centrosome), and Golgin245 (trans-Golgi). Arrowheads indicate centrosomes. Experiment repeated 4 times with similar results. Main scale bar,5 μm; Inset scale bar, 0.5 μm.

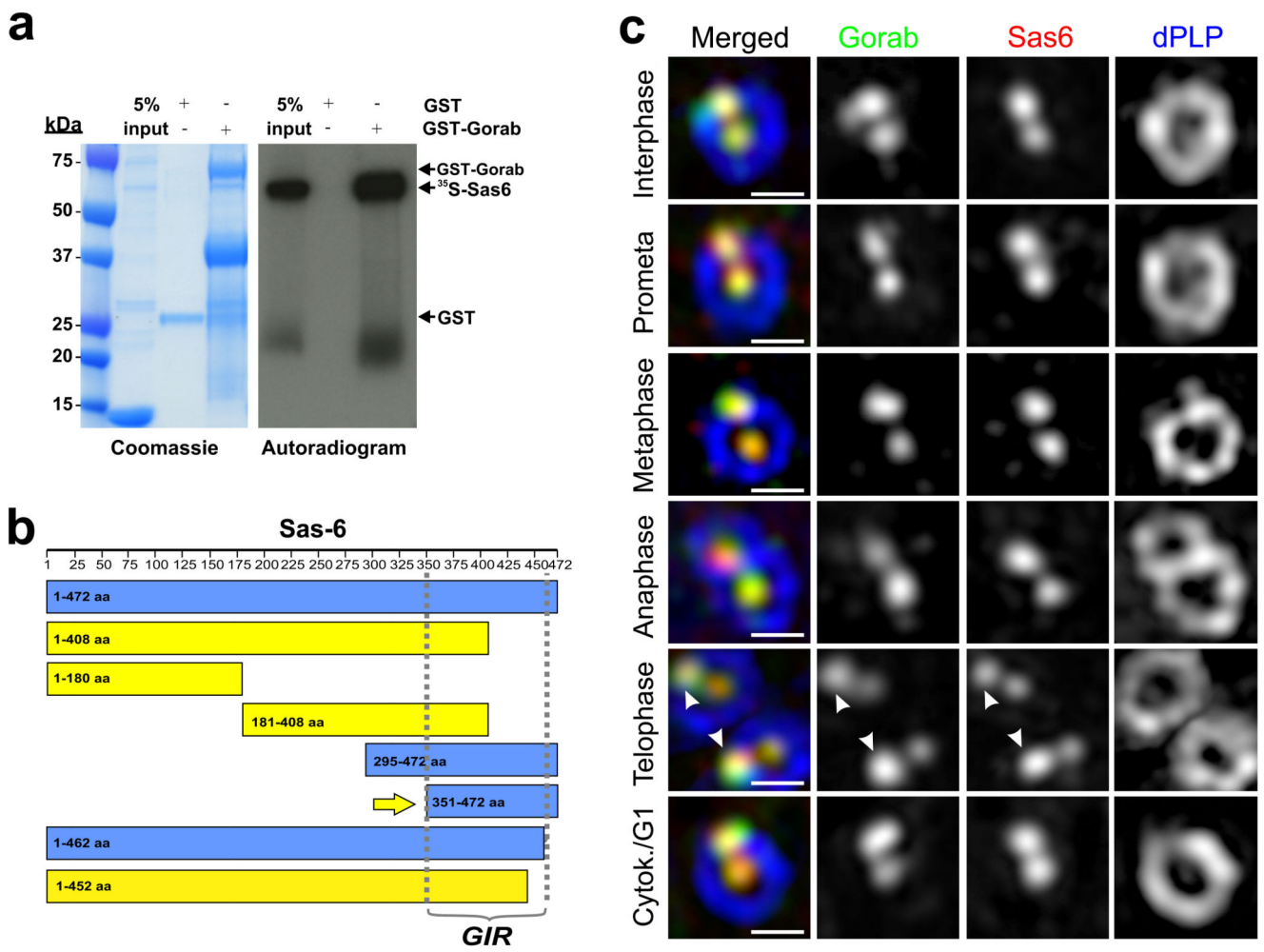

Fig. 2. Gorab directly interacts and colocalises with Sas6.

(**a**)*In vitro* assay of the Gorab-Sas6 interaction. GST-Gorab was incubated with ^{35}S-Methionine-labelled Sas6 and resulting complexes subjected to SDS-PAGE and autoradiography. Experiment repeated 3 times with similar results (**b**) Schematic of Sas6 indicating fragments interacting (blue) or not interacting with Gorab (yellow). Arrow, minimal interacting fragment (GIR: Gorab Interacting Region). (**c**) 3D-SIM localization of endogenous Gorab (green) and Sas6 (red) throughout the D-Mel2 cell cycle relative to zone III marker, dPLP (blue). Arrowheads, site of procentriole formation. Experiment repeated 2 times with similar results. Scale bars,250 nm.

Europe PMC Funders Author Manuscripts

Europe PMC Funders Author Manuscripts

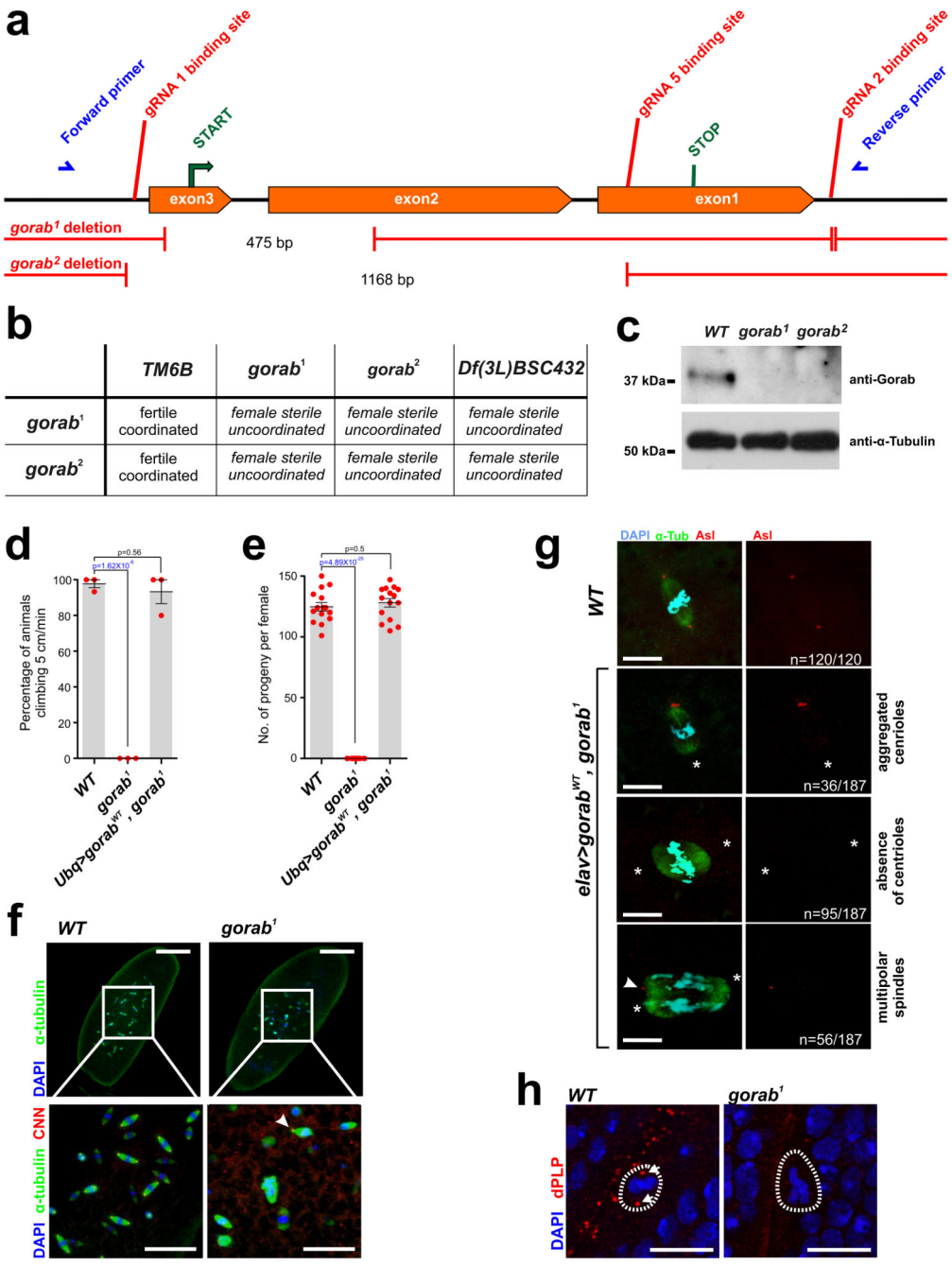

Fig. 3. *gorab* null mutant flies show female sterility and coordination defects.

(**a**) Schematic of *gorab* gene showing guide RNA binding sites (red) for CRISPR/Cas9 mutagenesis and primer binding sites for detection and sequencing of indicated *gorab*^{1} and *gorab*^{2} deletion mutants (blue). (**b**) Complementation tests for female fertility and coordination. 200 individuals tested per genotype. (**c**) Western blot of extracts from 5 adult females of indicated genotypes. Gorab revealed by antibody raised against its N terminal fragment (see Online Methods). α-tubulin, loading control. Experiment repeated once with similar result. (**d**) Climbing ability of wild type, *gorab*^{1}and rescued (N-terminal-GFP-tagged

Europe PMC Funders Author Manuscripts

gorab^{WT} cDNA expressed from ubiqutin promoter in *gorab*^{1} background) flies raised at 29 °C. Cohorts of 15 flies scored for number climbing 5 cm in 1 min.); Means ± s.e.m are shown for N=3 independent experiments, n= 15 flies/genotype investigated in each experiment. p values of two tailed unpaired t-tests are shown. p value in blue indicates significant difference (99% confidence interval) (**e**) Fertility of wild type, *gorab*^{1}and rescued (as in **d**) females individually mated with wild type males at 25°C over 6 days. Data points represent number of progeny of individual females. Means ± s.e.m are shown for n=15 females per genotype. p values of two tailed unpaired t-tests are shown. p value in blue indicates significant difference (99% confidence interval). Experiment repeated once with similar result. (**f**) Embryos from wild-type and *gorab*^{1}mutant mothers stained to reveal α-tubulin (green), centrosomin (CNN, red), and DNA (blue).; n=100 embryos were observed per genotype in two independent replicate experiments with similar results. Arrowhead, single centrosome of monopolar spindle. Scale bar, 100 μm (upper panel); 35 μm (lower panel). (**g**) Embryos from *elav>gorab*^{WT}*,gorab*^{1} mothers stained to reveal α-tubulin (green), asterless (Asl, red), and DNA (blue). Arrowhead, third pole of a multipolar spindle; asterisks, spindle poles lacking centrioles. Scale bar, 10 μm. (**h**) Wing discs from wild type and *gorab*^{1} larvae immunostained against dPLP to reveal centrosomes (red).Experiment repeated 3 times with similar results. Dashed lines, mitotic cells; Arrows, mitotic centrosomes. Scale bar,10 μm.

Europe PMC Funders Author Manuscripts

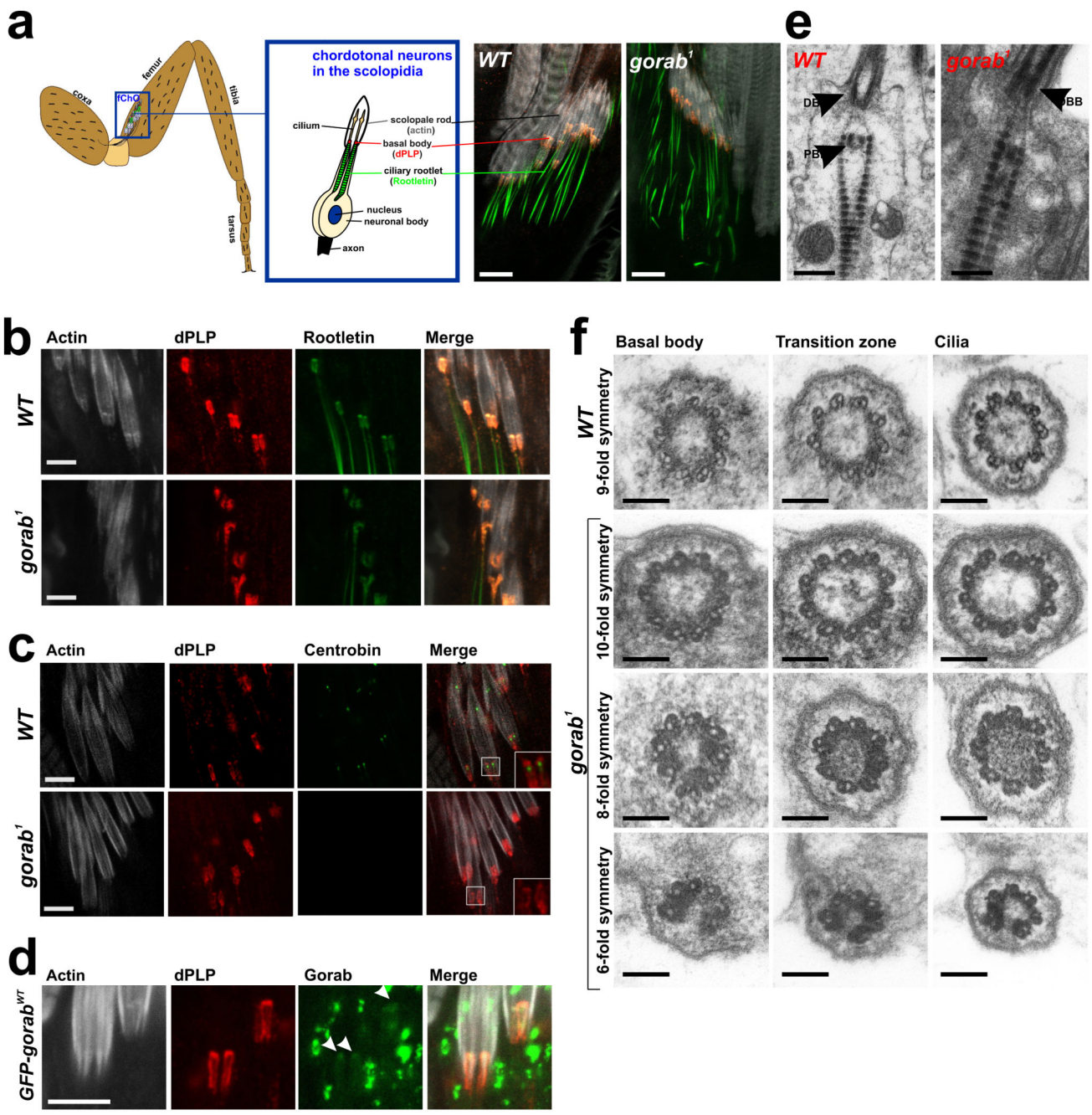

Fig. 4. Loss of daughter centriole and asymmetrical mother centrioles in *gorab* mutant ciliated neurons

(**a**)Schematic of femoral chordotonal organs (fChO) and stained, in wild type and *gorab*^{1} mutant, to reveal transgenic Rootletin-GFP (green), dPLP in basal bodies (red), and actin in scolopale rods (white). Experiment repeated twice with similar results. Scale bar,10 μm. (**b**) Detail of basal body organisation in wild-type and *gorab*^{1} stained as in a).Experiment repeated twice with similar results. Scale bar,10 μm. (**c**) Localisation of daughter centriole specific YFP-Centrobin (Cnb, green) in wild-type and *gorab*^{1}fChO basal bodies also stained

to reveal dPLP (red) and Actin (grey). Experiment repeated twice with similar results. Scale bar, 10 μm. (**d**) Localization of GFP-tagged Gorab expressed in *gorab*^{1} mutant background. Arrowheads, GFP-Gorab at basal bodies. Experiment repeated with similar result. Scale bar, 10 μm. (**e**) EM images of longitudinal sections wild-type and *gorab*^{1}fChOs. n= 11 ciliated cells were scored. Arrowheads, distal (DBB) and proximal (PBB) basal bodies. Scale bar, 0.2 μm. (**f**) Transverse sections of basal bodies, transition zones and cilia in wild-type and *gorab*^{1}imaged by TEM. n=16 ciliated cells were scored.Scale bar, 0.1 μm.

Europe PMC Funders Author Manuscripts

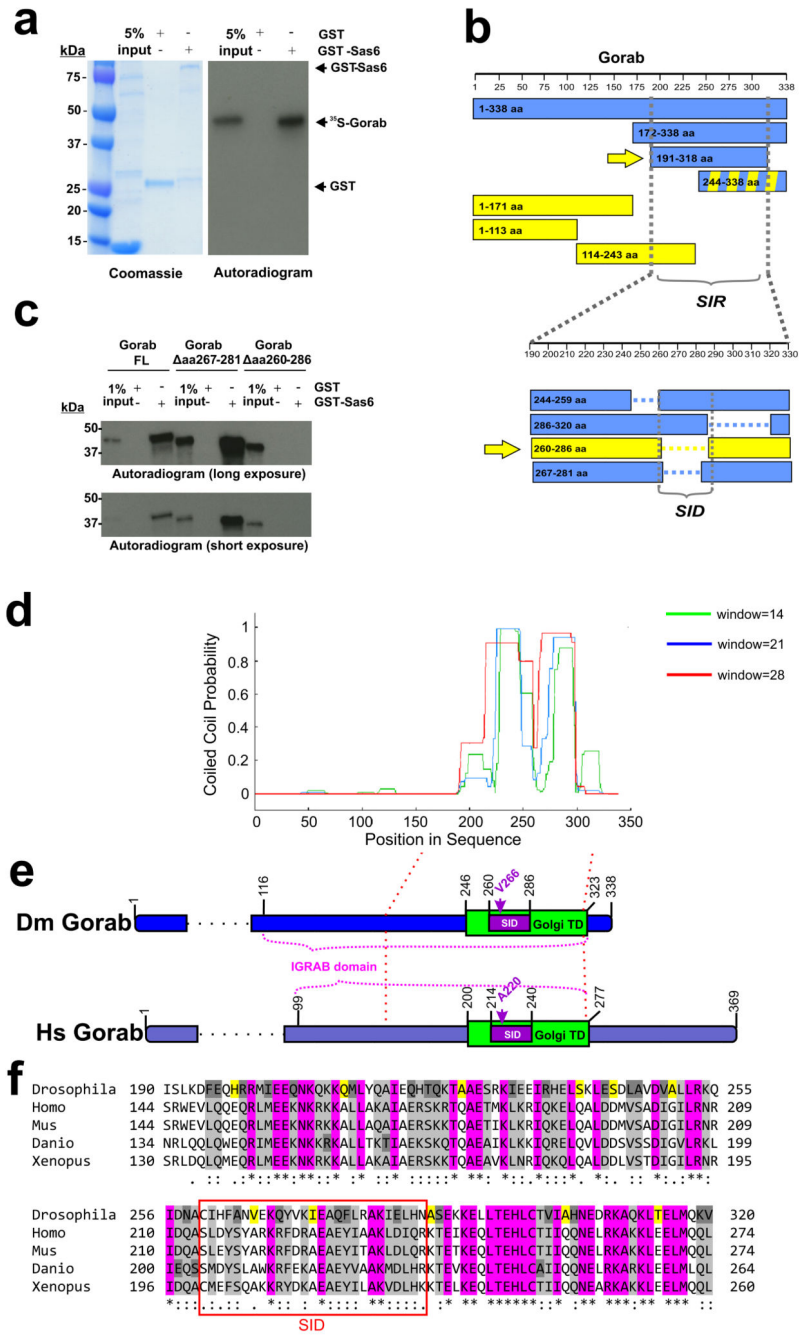

Fig. 5. Domain structure of Gorab.

(**a**) *In vitro* interaction of GST-Sas6 and ^{35}S-Methionine-labelled Gorab. Experiment repeated 2 times by different investigators with similar result. (**b**) Identification of minimal Sas6 interacting region (SIR) in Gorab (upper panel). Green bars, Gorab fragments interacting with Sas6. Red bars, Gorab fragments not interacting with Sas6. Green and red stripes, weak interaction. Arrow indicates minimal interacting fragment. Minimal Gorab deletion that abolishes Sas6 interaction (lower panel). Green bars, Sas6 interacting Gorab constructs; red bars, non-interacting constructs. Arrow, minimal deletion abolishing the

interaction with Sas6, the Sas6 interacting domain (SID). (**c**) Sas6 interaction with ^{35}S-Methionine-labelled full length (FL) Gorab and indicated deletion variants. Experiment repeated independently by different investigator with similar result.(**d**) Prediction of coiled-coil region in Gorab, by Coils server by scanning windows of 14, 21 and 28 residues.(**f**) Comparison of domain topologies of *Drosophila* and human Gorab. Sas6 interacting domain (SID, purple), Golgi targeting domain (Goldi TD, green), and IGRAB domain are indicated. (**g**) Alignment of predicted coiled-coil region of *Drosophila* Gorab and five vertebrate species homologues. Pink, amino acids conserved between all; grey, similar amino acid groups; dark grey, single divergent amino acids; and yellow, a single divergent amino acid in *Drosophila*. Alignment generated with Clustal Omega. Purplebox, SID.

Europe PMC Funders Author Manuscripts

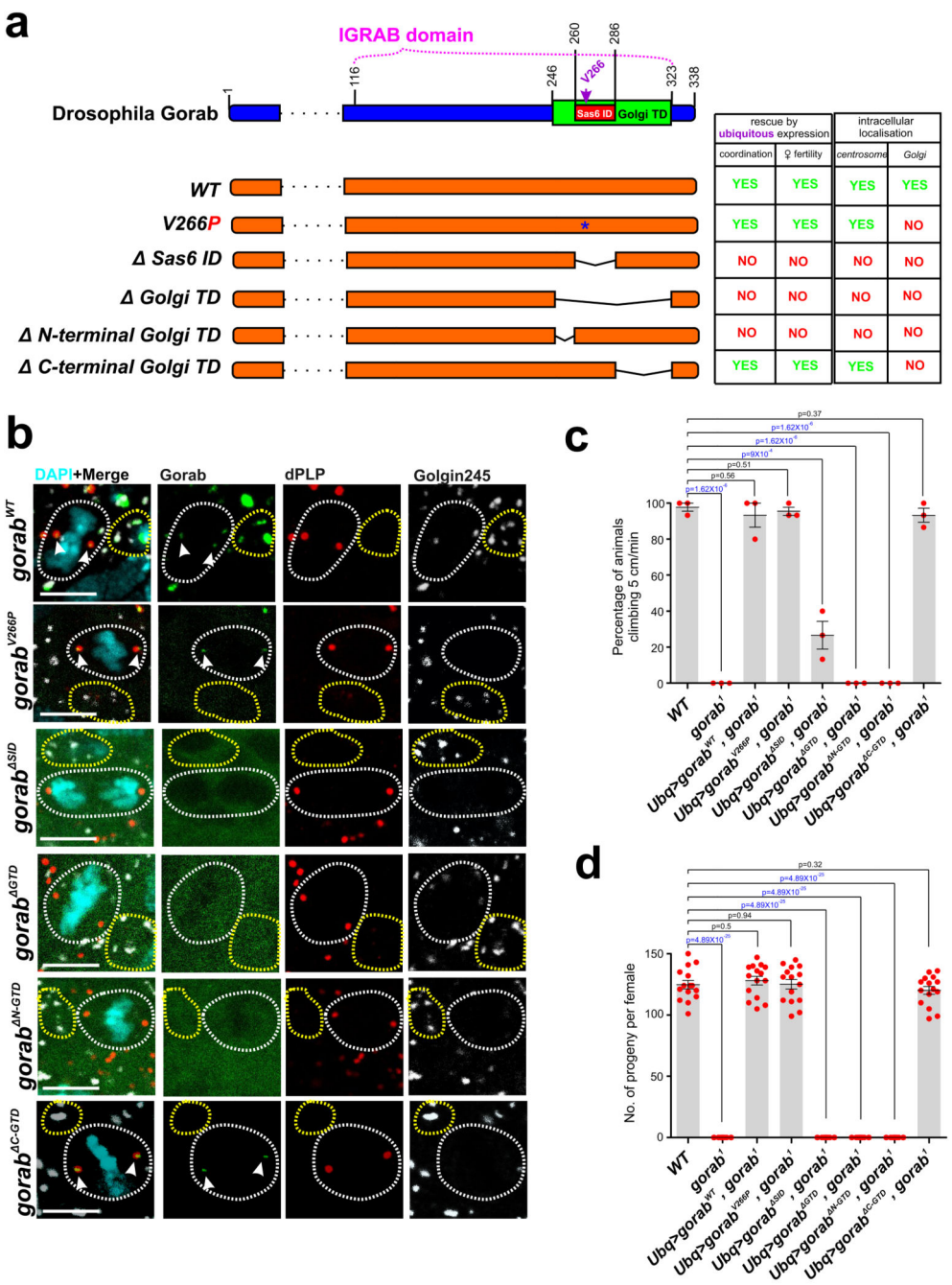

Fig. 6. Functional Domains of Gorab.

(**a**)Schematic of mutant *gorab* transgenes used in localization and rescue experiments. Asterisk, position of Val266 to Pro substitution. Gaps connected with thin line indicate extents of deletions. Tables summarizes rescue and localization experiments alongside indicated mutant forms. (**b**)Intracellular localization of Gorab mutant transgene products, Wing discs from larvae expressing the indicated GFP-tagged Gorab mutant protein stained to reveal dPLP (red) and Golgin245 (grey). White dashed lines, mitotic cells; yellow dashed lines, interphase cells with assembled Golgi. Experiments repeated 3 times with similar

Europe PMC Funders Author Manuscripts

results. Arrowheads, centrosomes of mitotic cells. Scale bar, 5μm. (**c**) Rescue of climbing ability by ubiquitous expression of indicated N-terminally GFP-tagged transgene in *gorab*^{1} flies raised at 29 °C. Means ± s.e.m for N=3 experiments, n= 15 flies/genotype per experiment. p values of two tailed unpaired t-tests are shown. p value in blue indicates significant difference (99% confidence interval) (**d**) Rescue of female sterility by ubiquitous expression of indicated N-terminally GFP-tagged transgenes in *gorab*^{1} background.Data points represent the number of progeny of individual females. Mean ± s.e.m are shown for n=15 females per genotype. p values of two tailed unpaired t-tests are shown. p value in blue indicates significant difference (99% confidence interval). Experiment repeated once with similar result.

Europe PMC Funders Author Manuscripts

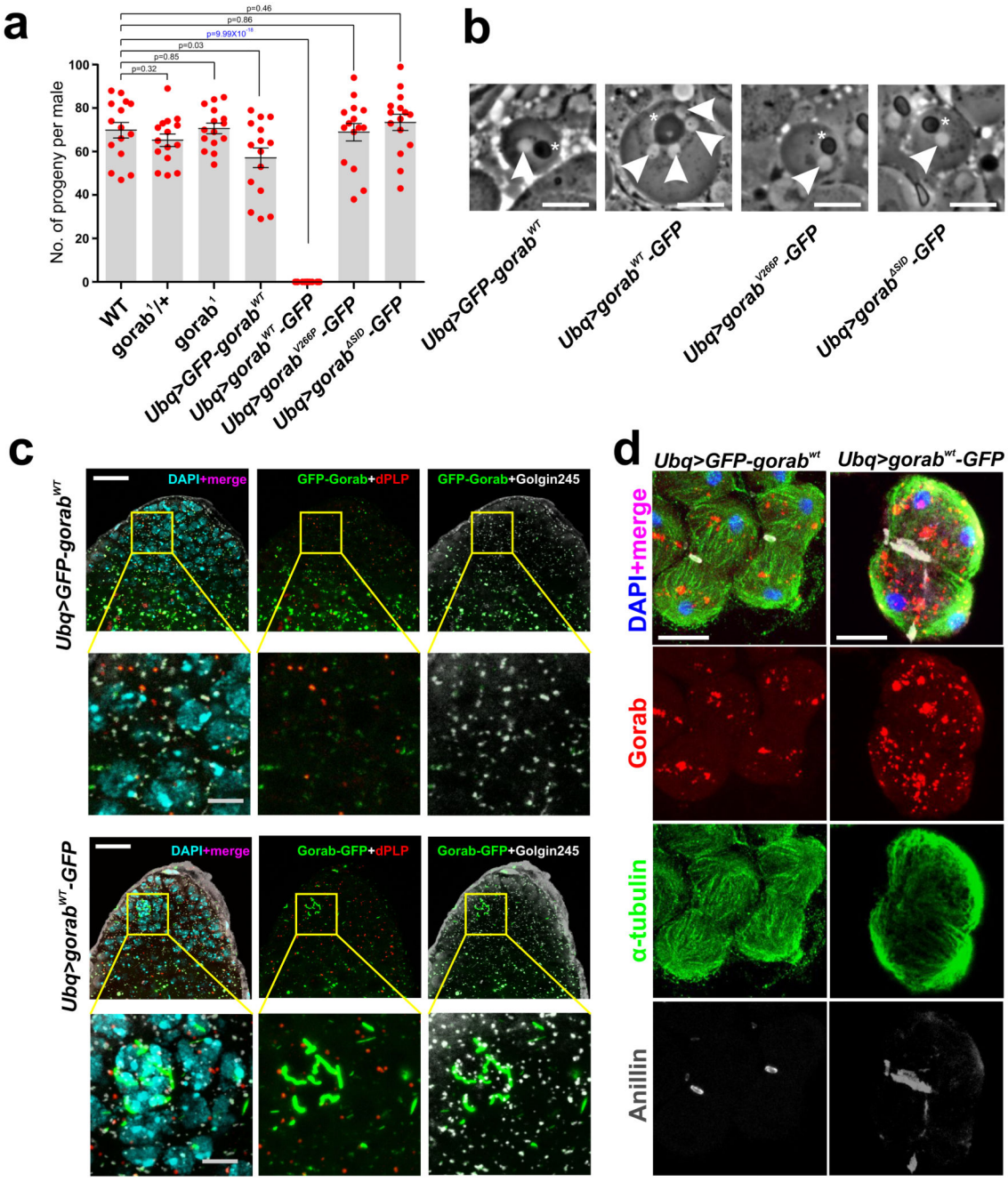

Fig. 7. Dominant male sterility and cytokinesis defects upon expression of C-terminally GFP tagged Gorab.

(**a**) Fertility of wild type, *gorab*^{1} males and males expressing indicated transgenes. Data points represent the number of progeny of individual males. Means ± s.e.m are shown for n=15 males per genotype. p values of two tailed unpaired t-tests are shown. p value in blue indicates significant difference (99% confidence interval). Experiment repeated once with similar result(**b**) Phase contrast micrographs of spermatids from males expressing indicated transgenes. Arrowheads indicate nuclei; asterisk, the mitochondrial derivative Nebenkern.

Europe PMC Funders Author Manuscripts

Experiment repeated 3 times with similar results. Scale bar, 10 μm. (**c**) Apical parts of testes from males expressing N- or C-terminally GFP-tagged Gorab and stained to reveal dPLP (red) and Golgin245 (grey). Experiment repeated 2 times with similar results. Scale bars, 20 μm and 5μm (inset). (**d**) Spermatocytes in meiotic telophase from of males expressing N- or C-terminally GFP-tagged Gorab (red) and stained to reveal tubulin (green), anillin (white) and DNA (blue). Experiment repeated 2 times with similar results. Scale bar, 10 μm.

Europe PMC Funders Author Manuscripts

Table 1

Copurification of Drosophila Sas6 and Gorab.

(top) Co-purification of Gorab with GFP-Sas6 from polyUbiquitin-Sas6-GFP *Drosophila* embryos or Protein A-Sas6 expressed from metallothionein promoter in D.Mel-2 cells. Extracts made in isotonic or high salt (440mM NaCl) buffer and with okadaic acid (OA) and MG132 as indicated (Materials and Methods). Proteins commonly identified in control purifications of GFP or other GFP-tagged proteins are excluded but given in tables S1A-E. Scores (Mascot) and numbers of peptides detected by mass spectrometry are indicated. (bottom) Affinity purification of tagged Gorab from poly-Ubiquitin-GFP-Gorab Drosophila embryos or D.Mel-2 cells stably transformed with poly-Ubiquitin-GFP-Gorab or p-metallothionein (pMT)-GFP-Gorab (induced with 1mM CuSO4 for 22h). Co-purifying Sas6 and COPI complex proteins selected from the full list of co-purified proteins in tables S2 A-E.

	Syncytial embryos						Cultured cells			
	pUb-Sas6-GFP		pUb-Sas6-GFP (+440mM NaCl)		pUb-Sas6-GFP (+440mM NaCl;OA)		pMT-PrA-Sas6 (+MG132)		pMT-PrA-Sas6 (+MG132; OA)	
Proteins identified	**Score**	**Peptides**	**Score**	**Peptides**	**Score**	**Peptides**	**Score**	**Peptides**	**Score**	**Peptides**
Sas6	13751	272	5900	123	4677	131	4576	281	4606	280
Gorab	6514	105	1641	27	1380	27	69	5	55	2

	Syncytial embryos		Cultured cells							
	pUb-GFP-Gorab		pUb-GFP-Gorab		pUb-GFP-Gorab (+ OA)		pMT-GFP-Gorab		pMT-GFP-Gorab (+ OA)	
Proteins identified	**Score**	**Peptides**	**Score**	**Peptides**	**Score**	**Peptides**	**Score**	**Peptides**	**Score**	**Peptides**
Gorab	2764	50	18036	290	61897	766	16669	253	24140	337
Sas6	752	18	159	4	1961	37	253	2	337	7
αCOP	-	-	1106	26	606	13	72	2	329	11
β'COP	-	-	322	8	212	3	336	4	441	6
βCOP	-	-	1263	19	582	9	259	4	590	12
γCOP	-	-	1792	29	1171	22	109	3	488	8
δCOP	-	-	-	-	-	-	-	-	-	-
εCOP	-	-	96	2	92	2	-	-	138	1
ζCOP	-	-	-	-	-	-	-	-	-	-